2024 6th International Conference on Electrical Engineering and Information & Communication Technology (ICEEICT)
02-04 May 2024, Military Institute of Science and Technology (MIST), Dhaka-1216, Bangladesh

2024 6th International Conference on Electrical Engineering and Information & Communication Technology (ICEEICT) | 979-8-3503-8577-9/24/$31.00 ©2024 IEEE | DOI: 10.1109/ICEEICT62016.2024.10534543

OTFS-Aided Waveform Design for MU-MIMO Joint Sensing and Communication Systems

Rafiul Kadir
ECE Discipline
Khulna University
Khulna-9208, Bangladesh
Email: ku.rafiul@gmail.com

Mohammad Ismat Kadir
ECE Discipline
Khulna University
Khulna-9208, Bangladesh
Email: ismat.kadir@ece.ku.ac.bd

***Abstract*—An orthogonal time frequency space (OTFS) modulation-based joint sensing and communication (JSAC) system is proposed. A multi-user multi-input multi-output (MU-MIMO) system is also considered for the JSAC system. OTFS can mitigate the channel-induced dispersion, while the OTFS signal has a low peak-to-average power ratio (PAPR). OTFS is a modulation scheme where delay-Doppler domain transmit grids are formed by appropriately mapping the constellation symbols. OTFS is capable of providing significant advantages in challenging scenarios with severe fading, delay spread, and Doppler shift. The proposed OTFS-based dual-functional waveform optimizes spectral efficiency by sharing the same frequency band and enhances the overall performance of the MU-MIMO JSAC scheme. The performance of the OTFS-based MU-MIMO JSAC has been investigated in terms of ambiguity function, sum rate, and range-angle response. The proposed OTFS MU-MIMO JSAC provides remarkable performance compared to the traditional JSAC system.**

***Index Terms*—OTFS, delay-Doppler, joint sensing and communication (JSAC), MU-MIMO.**

I. Introduction

Joint sensing and communication (JSAC) systems have attracted substantial research interest in recent years. By combining sensing capabilities with robust communication infrastructure, JSAC optimizes efficiency and responsiveness in a dynamic environment. The JSAC system combines radar sensing and communication functionalities. The sensing system aims to generate several transmit beams for sensing applications while communication components aim to transmit communication symbols to downlink users. Radar system requires a high frequency and a large bandwidth to attain high resolution, while communication systems also need a large bandwidth for high data transmission rates. So, the message signal is embedded with radar waveform for facilitating JSAC without requiring additional bandwidth. As a further advance, multiple-antenna-based radar has great potential and can provide diversity to achieve improved resolution, and accuracy in target detection. MIMO radar transmits multiple probing signals [1]. The degrees of freedom obtained by using multiple antennas are more than that attainable by using phased-array radars.

Since the same frequency band is used for both the sensing and communication functions, the high cost of spectrum and hardware is reduced with the aid of JSAC. From the implementation viewpoint, radio-frequency front-end structures have been developed, and a joint radio frequency hardware platform can be realized. With the increasing demand for JSAC, the challenging requirements in high-mobility scenarios characterized by high Doppler shifts are also increasing. JSAC in terms of practical implementation and integrated waveform design has been comprehensively studied in several pieces of literature. Specifically, JSAC using OFDM was investigated in [2]. OFDM signals have a high peak-to-average power ratio (PAPR). Additionally, OFDM can not overcome the channel impairments due to a high Doppler spread.

At this stage, orthogonal time-frequency space (OTFS) modulation emerged. OTFS is capable of providing enhanced performance in hostile doubly selective wireless channels. OTFS has a lower PAPR than OFDM and is capable of combating fading in wireless channels. OTFS diverges from conventional methods of symbol mapping onto either the time or frequency domain by instead mapping symbols onto the delay-Doppler (DD) domain. OTFS can handle strict and challenging requirements of large Doppler shifts, high data rate, ultra-high reliability, dense connectivity, high energy, and spectral efficiency of wireless systems. In consideration of the DD-domain symbol mapping, OTFS-based modulation appears to be promising for the next-generation JSAC systems. Specifically, the 6G wireless system is expected to enable the forthcoming Internet of Things (IoT) services. OTFS-based JSAC has also been considered. Low complexity OTFS plus frequency-modulated continuous wave (FMCW) waveform was designed for JSAC in [3]. However, the dynamic range of the JSAC scheme may suffer as a result of this integrated design. This is mostly caused by the high downlink pilot overhead, which increases with the channel's maximum Doppler spread, maximum delay spread, and number of antennas at the transmitter [4]. However, an integrated JSAC in a multi-user or multi-antenna system is still unexplored.

Against this backdrop, we propose an OTFS waveform for a multiuser multiple-input multiple-output (MU-MIMO) JSAC scenario. The scheme proposed in this paper can effectively provide simultaneous sensing and communication functionality in an MU-MIMO system even under a hostile doubly selective channel scenario.

979-8-3503-8577-9/24/$31.00 ©2024 IEEE

Authorized licensed use limited to: Khulna University. Downloaded on October 19,2026 at 07:23:03 UTC from IEEE Xplore. Restrictions apply.

We organize the remaining part of this paper as follows. Section II outlines the system architecture, while Section III describes the waveform design process. Section IV provides the results of our simulations. Finally, we conclude the paper in Section V.

II. System Overview

The proposed OTFS-based MU-MIMO JSAC architecture is portrayed in the schematic diagram of Fig. 1. The system shown in Fig. 1 facilitates the integration of sensing capabilities with a communication system using N_t transmit antenna K communications users and Q sensing targets. This section first outlines the transceiver architecture using OTFS modulation, which is then followed by a brief description of the MU-MIMO JSAC scheme considered. Finally, OTFS modulation-based waveform design of the proposed MU-MIMO JSAC is described.

A. JSAC transmitter using OTFS modulation

In the proposed JSAC system, there are two components within the same architecture - the communication component and the radar component. The communication part deals with the transmission of data or information over the channel, while the radar part is responsible for sensing applications. Each component sets different requirements for the transmitted waveform. To satisfy the requirements of the two simultaneous functionalities, the frequency spectrum becomes more congested as the number of linked devices increases. Therefore, we designed an OTFS modulated a set of dual-functional waveforms for embedded JSAC to increase the spectrum utilization. The proposed system is a MU-MIMO-OTFS JSAC system. As mentioned and as shown in Fig. 1, the system is equipped with N_t antennas, which provide service to K communication users each having a single antenna element. Each antenna in the OTFS-based MU-MIMO JSAC system transmits OTFS-modulated information symbols independently.

1) Implementation of OTFS modulation: First, the source bits are converted into symbols by employing a QPSK constellation. Then the resulting QPSK symbols are mapped into DD frames. The DD frames are two-dimensional (2D) frames comprising the data symbols. The mapped OTFS $M \times N$ data frame is denoted as $\boldsymbol{X}$. Specifically, M refers to the number of delay bins and N denotes the number of Doppler bins in the DD frames. After the symbol mapping, the mapped DD frames undergo an inverse symplectic finite Fourier transform (ISFFT) operation. As a result of this operation, the symbol frames are converted from DD domain to the time-frequency (TF) domain. Performing the ISFFT operation is equivalent to performing two Fourier operations. To be specific, this is implemented by first applying an M-point fast Fourier transform (FFT) to the columns of the DD frame, which is followed by an N-point inverse fast Fourier transform (IFFT) to the rows of the DD frames.

Secondly, the TF-domain signal is transformed into the baseband time domain (TD) signal $\boldsymbol{S(t)}$ with the aid of the Heisenberg transform. To achieve this, an M-point IFFT is employed and the signal is pulse-shaped using an appropriate waveform. The OTFS modulated information symbols $x(t)$ independently transmit through each antenna. For convenient manipulation and simple matrix multiplication-based system design for further analysis, let us denote M-point FFT by $\boldsymbol{F}_M$ and N-point IFFT by$\boldsymbol{F}_N^H$. Then, we can express the OTFS modulated TD signal in matrix form [5] by

$$\boldsymbol{S} = \boldsymbol{G}_{tx}\boldsymbol{F}_M^H(\boldsymbol{F}_M\boldsymbol{X}\boldsymbol{F}_N^H) = \boldsymbol{G}_{tx}\boldsymbol{X}\boldsymbol{F}_N^H, \tag{1}$$

where $\boldsymbol{G}_{tx}$ is the pulse-shape waveform matrix which is a diagonal matrix. Equation (1) is further simplified into vector form by column-wise vectorial stacking operation vec(•). Using this operation, we can express the TD matrix $\boldsymbol{S} \in \mathbb{C}^{M\times N}$ as a vector. Naturally, this vector $\boldsymbol{s}$ will be of dimension $MN \times 1$, which can be written as

$$\begin{aligned} \boldsymbol{s} &= \text{vec}\,(\boldsymbol{S}) \\ &= \left(\boldsymbol{F}_N^H \otimes \boldsymbol{G}_{tx}\right) \text{vec}\,(\boldsymbol{X}) \\ &= \left(\boldsymbol{F}_N^H \otimes \boldsymbol{G}_{tx}\right) \boldsymbol{x}. \end{aligned} \tag{2}$$

After that, $\boldsymbol{s} \in \mathbb{C}^{MN\times 1}$ is transmitted through the n^{th} transmit antenna ($n = 1, 2, \cdots, N_t$). Denoting the communication frame length by L, the transmit signal matrix is represented as $\boldsymbol{X_m}$, where m 'just' refers to the 'message' or communication signal. Since there are N_t transmit antennas, $\boldsymbol{X_m}$ can be seen as a $N_t \times L$ block matrix, each of whose elements are $MN \times 1$ TD symbol matrix due to the above-mentioned implementation of OTFS-based modulation. Thus the MIMO JSAC transmit signal matrix $\boldsymbol{X_m}$ can be written as

$$\boldsymbol{X_m} = \begin{bmatrix} x_{1,1} & x_{1,2} & \cdots & x_{1,L} \\ x_{2,1} & x_{2,2} & \cdots & x_{2,L} \\ \vdots & \vdots & \ddots & \vdots \\ x_{N_tMN,1} & x_{N_tMN,2} & \cdots & x_{N_tMN,L} \end{bmatrix}. \tag{3}$$

Here, we emphasize that the communication signal frame $\boldsymbol{X_m} \in \mathbb{C}^{N_tMN\times L}$ will be used as the dual-functional waveform matrix, where $x_{n,j}$ represents the signal from the n^{th} transmit antenna at the j^{th} instance. Each column of $\boldsymbol{X_m}$ corresponds to the transmitted signals at a specific time, and the entire matrix provides a complete picture of the signals throughout the entire frame.

2) Doubly Selective Channel Model: We assume the complex baseband channel impulse response (CIR) for each link to be doubly selective. We consider integer delay and Doppler shift. So, the delay and Doppler for the t^{th} path defined as $\tau_t = \frac{l_{\tau_t}}{M\delta f}$ and $\upsilon_t = \frac{q_{\upsilon_t}}{NT}$, where l_{τ_t} and q_{υ_t} denote the delay and Doppler indices corresponding to the t^{th} path. Denoting the TD additive white Gaussian noise (AWGN) by $w(t)$, the received signal can be written [5] as

$$y(t) = \int_{\upsilon}\int_{\tau} h(\tau,\upsilon)s(t-\tau)e^{j2\pi\upsilon(t-\tau)}\,\mathrm{d}\tau\,\mathrm{d}\upsilon + w(t). \tag{4}$$

Equation (4) can be represented in simple matrix form for

Authorized licensed use limited to: Khulna University. Downloaded on October 19,2026 at 07:23:03 UTC from IEEE Xplore. Restrictions apply.

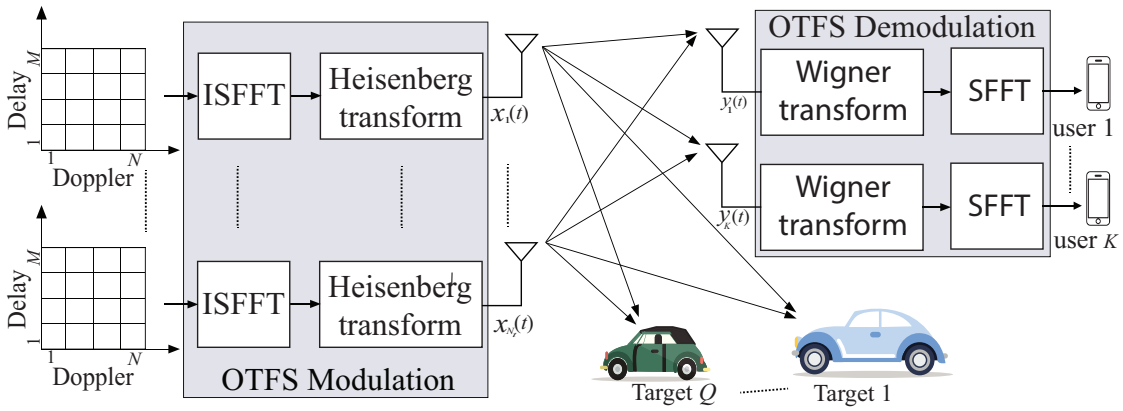


Fig. 1. Block diagram of the OTFS-based MU-MIMO JSAC system.

the TD received signal as

$$\boldsymbol{y} = \breve{\boldsymbol{H}}\boldsymbol{s} + \boldsymbol{w}, \tag{5}$$

where the channel matrix may be written [5] as

$$\breve{\boldsymbol{H}} = \sum_{t=1}^{T_p} h_t \boldsymbol{\Psi}^{l_t} \boldsymbol{\Omega}^{(k_t)} \in \mathbb{C}^{MN \times MN}. \tag{6}$$

The channel transfer matrix $\breve{\boldsymbol{H}}$ is a circulant matrix, composed of the channel's delay matrix $\boldsymbol{\Psi}$ characterized by the circular shifts of the channel transfer function, and the Doppler matrix $\boldsymbol{\Omega}^{(k_t)}$. More precisely, $\boldsymbol{\Psi}$ and $\boldsymbol{\Omega}^{(k_t)}$ denote the delay-related permutation matrix and the mobility-induced Doppler matrix, respectively. The form of the $MN \times MN$ permutation matrix is given [5] by

$$\boldsymbol{\Psi} = \begin{bmatrix} 0 & \cdots & 0 & 1 \\ 1 & \ddots & 0 & 0 \\ \vdots & \ddots & \ddots & \vdots \\ 0 & \cdots & 1 & 0 \end{bmatrix}$$

and the Doppler matrix $\Omega^{(k_t)} \in \mathbb{C}^{MN \times MN}$ is expressed [5] as

$$\boldsymbol{\Omega}^{(k_t)} = \begin{bmatrix} e^{\frac{j2\pi k_t(0)}{MN}} & 0 & \cdots & 0 \\ 0 & e^{\frac{j2\pi k_t(1)}{MN}} & \cdots & 0 \\ \vdots & & \ddots & \vdots \\ 0 & 0 & \cdots & e^{\frac{j2\pi k_t(MN-1)}{MN}} \end{bmatrix}.$$

Furthermore, the channel gain associated with the t^{th} path is denoted as h_t.

3) OTFS Detection and Demodulation: The receiver demodulates the time-domain (TD) signal using OTFS. Subsequently, the TD signal received is transformed into the DD signal. To demodulate the signal, the TD received signal expressed by y is initially de-vectorized into the matrix $\boldsymbol{Y}\mathbb{C}^{M\times N}$. The de-vectorized form can be expressed as $\boldsymbol{Y} = vec^{-1}(y)$. We use the Wigner transform on the de-vectorized matrix $\boldsymbol{Y}$ to transfer it into the TF domain signal matrix. Then symplectic Fourier transform (SFFT) operation is applied to shift it again to the DD domain. The DD domain signal may be written [5] as

$$\tilde{\boldsymbol{X}} = \boldsymbol{F}_M^H(\boldsymbol{F}_M \boldsymbol{Y})\boldsymbol{F}_N^H$$

B. Communication Regime

The matrix representing the received multiple-user signal matrix can be written as

$$\boldsymbol{Y}_K = \boldsymbol{H}\boldsymbol{X}_{\boldsymbol{m}} + \boldsymbol{W}, \tag{7}$$

where $\boldsymbol{W}$ and $\boldsymbol{Y}_K$ are the noise matrix and received signal, respectively. From the MU-MIMO input-output relationship of users K. Due to modulo operations, the matrix $\boldsymbol{H}$ is sparse - each row and column contains only a few non-zero elements as dictated by the number of channel taps. We further note that $\boldsymbol{H} \in \mathbb{C}^{KMN \times N_t MN}$ is the MU-MIMO channel matrix described by

$$\boldsymbol{H} = \begin{bmatrix} \boldsymbol{H}_{1,1} & \boldsymbol{H}_{1,2} & \cdots & \boldsymbol{H}_{1,N_t} \\ \boldsymbol{H}_{2,1} & \boldsymbol{H}_{2,2} & \cdots & \boldsymbol{H}_{2,N_t} \\ \vdots & \vdots & \ddots & \vdots \\ \boldsymbol{H}_{K,1} & \boldsymbol{H}_{K,2} & \cdots & \boldsymbol{H}_{K,N_t} \end{bmatrix} \tag{8}$$

where each $\boldsymbol{H}_{k,n_t} \in \mathbb{C}^{MN \times MN}$.

The signal matrix $\boldsymbol{X}_{\boldsymbol{m}}$ entails both radar and communication functionalities and hence is used as a dual-functional waveform [6], [7]

We can rewrite the intended user's received signal as the matrix of constellation symbols $\boldsymbol{C} \in \mathbb{C}^{KMN \times L}$ as follows

$$\boldsymbol{Y}_K = \boldsymbol{C} + (\boldsymbol{H}\boldsymbol{X}_{\boldsymbol{m}} - \boldsymbol{C}) + \boldsymbol{W}. \tag{9}$$

Since we assume each of the users employs the same constellation, the entries are taken from it. The term $(\boldsymbol{H}\boldsymbol{X}_{\boldsymbol{m}} - \boldsymbol{C})$ refers to the multiuser interference (MUI). We can calculate the energy corresponding to the MUI term [7] as

$$P_{T,MUI} = \| \boldsymbol{H}\boldsymbol{X}_{\boldsymbol{m}} - \boldsymbol{C} \|_F^2. \tag{10}$$

From (10), we see that the achievable sum rate and the total MUI energy are inter-related.

Authorized licensed use limited to: Khulna University. Downloaded on October 19,2026 at 07:23:03 UTC from IEEE Xplore. Restrictions apply.

C. Sensing Regime

We employ the MIMO radar system as a sensing component in the JSAC system. It is well known that MIMO radar is well-suited for sensing applications because it provides more information (DoFs) than conventional phased-array radars. For designing the waveform, the covariance matrix is first evaluated from the given beam pattern [7].

Specifically, given that the normalized spacing between adjacent antennas concerning the wavelength is d and the detection angle is θ, the transmit antenna's steering vector $\mathrm{a}(\theta)$ can be written [7] as follows:

$$\mathrm{a}(\theta) = [1, e^{j2\pi dsin\theta}, \cdots, e^{j2\pi(N_tMN-1)dsin\theta}]^T, \tag{11}$$

where we have $\mathrm{a}(\theta) \in \mathbb{C}^{N_tMN\times 1}$.

Denoting the spatial covariance matrix as $\boldsymbol{R_{dx}}$, the beam pattern can then be expressed by $\mathrm{P}(\theta)$=$\mathrm{a}^H(\theta)\boldsymbol{R_{dx}}\mathrm{a}(\theta)$, where .

Convex optimization may be used to construct such a beam pattern [1]. To design $\boldsymbol{X_m}$, we employ the spatial covariance matrix $\boldsymbol{R}_{dx}$ which can be expressed [7] as

$$\boldsymbol{R}_{dx} = \frac{1}{L}\boldsymbol{X_m}\boldsymbol{X_m}^H. \tag{12}$$

This relationship indicates that creating the waveform's covariance matrix corresponds to designing the transmit beam pattern for a MIMO radar. After that, we will design our proposed waveform based on the covariance matrix $\boldsymbol{R}_{dx}$.

D. Covariance matrix design from desired beam pattern

As mentioned above, the waveform is designed using the covariance matrix. The waveform covariance matrix R_{dx} can be obtained by optimization. This minimizes the squared error between the desired beam pattern $P(\theta)$ and the actual beam pattern $A(\theta)$. Thus, the optimization problem can be formulated [7] as follows:

$$\begin{aligned} \min_{\boldsymbol{R}_{dx}} \int_\theta |P(\theta) - A(\theta)|^2 \cos(\theta) d\theta \\ s.t.\ diag(\boldsymbol{R}_{dx}) = \frac{P_T}{N_tMN} \\ \boldsymbol{R}_{dx} =\in \mathbb{S}_+^{N_tMN}, \end{aligned} \tag{13}$$

where $A(\theta) = \mathrm{a}^H(\theta)\boldsymbol{R}_{dx}\mathrm{a}(\theta)$.

III. Waveform Design for the JSAC

Here, the waveform design is considered for MIMO radar under total power constraints. The waveform is designed from the evaluated covariance matrix. The optimization problem mentioned below employs singular value decomposition (SVD) to find the optimal solution for the waveform.

An omnidirectional beam pattern is considered for designing a JSAC waveform. For such a beam pattern, the MUI energy is the objective function, which requires to be minimized. Accordingly, we formulate the problem [7] as:

$$\begin{aligned} \min_{\boldsymbol{X_m}} \parallel \boldsymbol{H}\boldsymbol{X_m} - \boldsymbol{C}\parallel_F{}^2 \\ s.t.\ \boldsymbol{R}_{dx} = \frac{P_T}{N_tMN}\mathbf{I}_{N_tMN}, \end{aligned} \tag{14}$$

where $\boldsymbol{C} \in \mathbb{C}^{KMN\times L}$, P_T and $\mathbf{I}_{N_tMN}$ is the constellation symbol matrix, total transmit power and $N_tMN \times N_tMN$ identity matrix, respectively. Using singular value decomposition (SVD), the simple closed-form global solution is given [7] by

$$\boldsymbol{X_m} = \sqrt{\frac{LP_T}{N_tMN}}\boldsymbol{U}\mathbf{I}_{N_tMN\times L}\boldsymbol{V}^H, \tag{15}$$

where we obtain $\boldsymbol{U}\in\mathbb{C}^{N_tMN\times N_tMN}$ and $\boldsymbol{V} \in\mathbb{C}^{L\times L}$ by the SVD of $\boldsymbol{HC}$ given by

$$\boldsymbol{U}\sum\boldsymbol{V}^H = \boldsymbol{HC}. \tag{16}$$

Still referring to (15), $\mathbf{I}_{N_tMN\times L}$ is a unitary matrix composed by an identity matrix of dimension $N_tMN \times N_tMN$ and a zero matrix of dimension $N_tMN \times (L - N_tMN)$.

Table I
Values of Simulation Parameters Used

Parameter	Its Value
JSAC-related parameters	
N_t	16
Number of users	4
Modulation order	4
Maximum Speed	100 Kmph
Carrier frequency	4×10^9 Hz
No. of channel paths	4
Used channel model	Doubly Dispersive Rayleigh channel
OTFS modulation related parameters	
M	24
N	12

IV. Results and Discussion

Here, we have investigated the performance of the OTFS-based JSAC MU-MIMO system by numerical simulations. The performance metrics for the proposed waveform design procedure are the ambiguity function, the sum rate, and the range versus angle response. We employ the QPSK constellation for communication users. We employ a uniform linear array (ULA) of $N_t = 16$ antenna elements. We assume a half-wavelength spacing between the adjacent antenna elements. Furthermore, the system is studied with $M = 4$, and $N = 4$. Table I shows the values of the JSAC-related and OTFS-related simulation parameters.

A. The ambiguity function

Fig. 2 shows the ambiguity function with zero-delay cut of both the OTFS-JSAC waveform and JSAC waveform.

Authorized licensed use limited to: Khulna University. Downloaded on October 19,2026 at 07:23:03 UTC from IEEE Xplore. Restrictions apply.

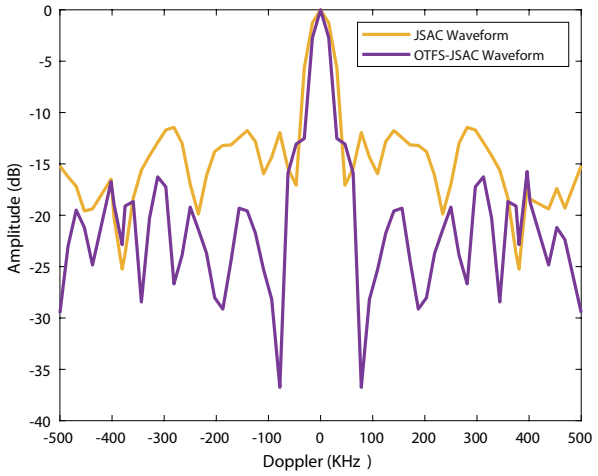


Fig. 2. Zero-delay cut of the ambiguity function. $N_t = 16$, and $K = 4$.

To be specific, the zero-delay cut waveform illustrates the targets' relative speed. As shown, the side lobe power of the MU-MIMO OTFS-JSAC waveform is considerably less than the waveform of conventional JSAC. Besides, better Doppler resolution is correlated with a narrower zero-delay cut. That means it is easier for the radar to discriminate between targets moving at various speeds. Thus, we can conclude that our proposed OTFS-based waveform is better suited for the MU-MIMO JSAC system than conventional JSAC over the high-mobility channel considered.

B. Range-Angle response

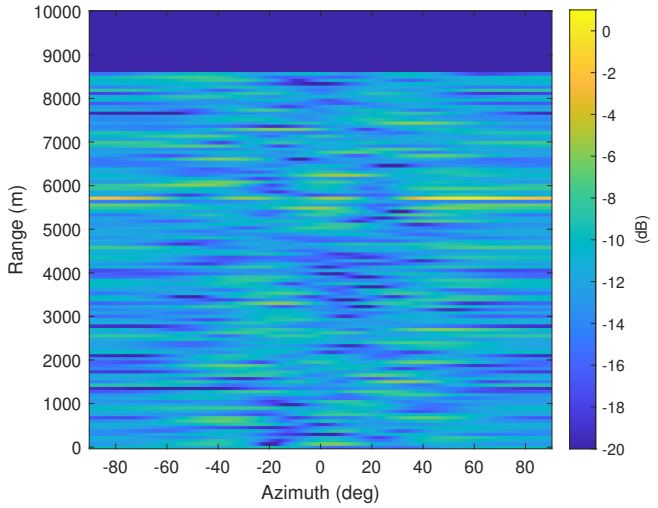
The range-angle response is a joint measure of how well the system can distinguish targets in both the range and angle domains [8]. It is often represented in a two-dimensional space, where one axis represents the range and the other represents the angle. The range-angle response is shown in Fig. 3. The range-angle response for the conventional JSAC system is shown in Fig. 3(a), while Fig. 3(b) provides the OTFS-JSAC range-angle response performance for $N_t = 16$ and $K = 4$. Three targets at angles and ranges of $-60^0, 0^0, 60^0$ and $6000\ m, 6230\ m, 5700\ m$, respectively, have been taken for the simulation. We observe that the proposed OTFS-JSAC can distinguish the three targets, while traditional JSAC cannot for the same doubly selective channel.

C. Sum-rate: A Trade-off between radar and communication Functionalities

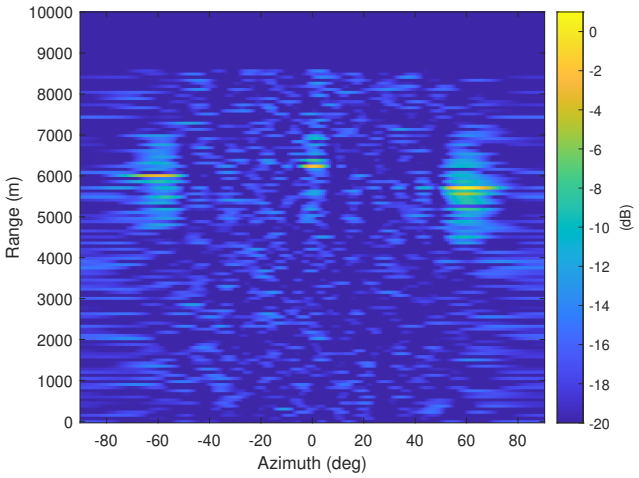
The achievable sum rate is a performance metric of the communication system which is defined by

$$\mathrm{R} = \sum_{i=1}^{K} \log_2(1 + \gamma_i), \tag{17}$$

In Fig. 4, the sum rate of the MU-MIMO JSAC is shown and compared with that of the MU-MIMO JSAC without OTFS modulation. Besides, the OTFS-based MU-MIMO system has



(a) Range-angle response of JSAC



(b) Range-angle response of OTFS-JSAC

Fig. 3. Performance comparison of range-angle response between OTFS-JSAC and traditional JSAC benchmark scheme, $N_t = 16$, $K = 4$

attained a 52 bps/Hz higher sum rate compared to the JSAC benchmark scheme over the doubly selective channel considered. The sum rate performance of conventional JSAC is seen to be very poor because the waveform struggles with the Doppler effect as well as MUI. OTFS can suppress the high Doppler effect and provide resilience to channel variance. Hence, OTFS modulation plays a significant role in improving the overall system performance. In OTFS, multiple devices located in different directions can communicate simultaneously without significant interference, making them suitable for crowded or dense deployment scenarios. This makes the proposed scheme a promising candidate for MU-MIMO JSAC.

V. Conclusion

An OTFS-based waveform and its design procedure have been proposed for MU-MIMO JSAC. First, the transmitted symbol matrix is organized in a delay-Doppler grid to form

Authorized licensed use limited to: Khulna University. Downloaded on October 19,2026 at 07:23:03 UTC from IEEE Xplore. Restrictions apply.

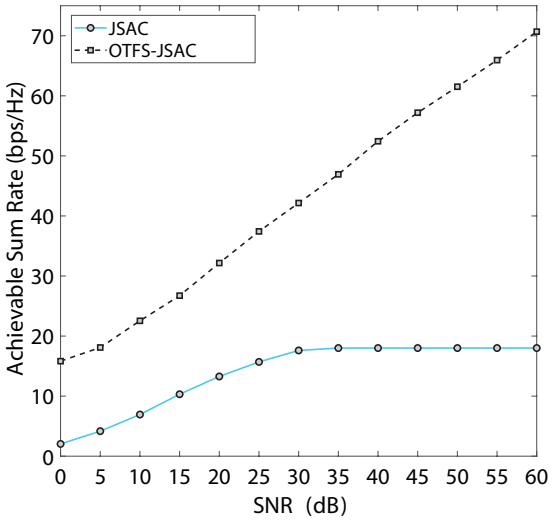


Fig. 4. Performance comparison in terms of sum-rate for different approaches, $N_t = 16$, $K = 4$.

a matrix to enable a dual-functional radar communication system. The transmit frame is considered to be transmitted over the MU-MIMO high-speed channel. The proposed OTFS-based MU-MIMO waveform and its performance have been studied in terms of ambiguity function, sum rate, and range-angle response. The proposed system is capable of detecting multiple targets at the same time while the communication sum rate is significantly high which represents our proposed system's robustness. Our proposed waveform is suitable for the MU-MIMO JSAC system over the high-speed channel.

VI. ACKNOWLEDGEMENT

The financial assistance of Khulna University for this work is gratefully acknowledged.

REFERENCES

[1] P. Stoica, J. Li, and Y. Xie, "On probing signal design for MIMO radar," *IEEE Trans. Signal Process.*, vol. 55, no. 8, pp. 4151–4161, 2007.

[2] S. N. Sur, P. Sharma, H. Saikia, S. Banerjee, and A. K. Singh, "OFDM-based radar-communication system development," *Procedia Computer Science*, vol. 171, 2020.

[3] S. E. Zegrar, S. Rafique, and H. Arslan, "OTFS-FMCW waveform design for low complexity joint sensing and communication," in *2022 IEEE 33rd PIMRC*. IEEE, 2022, pp. 988–993.

[4] M. F. Keskin, V. Koivunen, and H. Wymeersch, "Limited feedforward waveform design for OFDM dual-functional radar-communications," *IEEE Transactions on Signal Processing*, vol. 69, pp. 2955–2970, 2021.

[5] P. Raviteja, Y. Hong, E. Viterbo, and E. Biglieri, "Practical pulse-shaping waveforms for reduced-cyclic-prefix otfs," *IEEE Trans. Veh. Technol.*, vol. 68, no. 1, pp. 957–961, 2018.

[6] F. Liu, C. Masouros, A. Li, H. Sun, and L. Hanzo, "MU-MIMO communications with MIMO radar: From co-existence to joint transmission," *IEEE Trans. Wireless Commun.*, vol. 17, no. 4, pp. 2755–2770, 2018.

[7] F. Liu, L. Zhou, C. Masouros, A. Li, W. Luo, and A. Petropulu, "Toward dual-functional radar-communication systems: Optimal waveform design," *IEEE Trans. Signal Process.*, vol. 66, no. 16, pp. 4264–4279, 2018.

[8] R. Xi, C. Zheng, T. Huang, L. Wang, and Y. Liu, "Joint range and angle estimation for wideband forward-looking imaging radar," *IEEE Sensors J.*, vol. 22, no. 1, pp. 446–460, 2021.

Authorized licensed use limited to: Khulna University. Downloaded on October 19,2026 at 07:23:03 UTC from IEEE Xplore. Restrictions apply.